

Synthesis and Characterization of Cellulose Nanomaterials from Waste Newspapers [†]

Ziaul Hasan ^{1,2,*} , Md Osama Zubair ³  and Tauseef Hassan ³ ¹ Department of Biosciences, Jamia Millia Islamia, New Delhi 110025, India² Centre for Interdisciplinary Research in Basic Sciences, Jamia Millia Islamia, New Delhi 110025, India³ Center for Nanoscience and Nanotechnology, Jamia Millia Islamia, New Delhi 110025, India; osama.zubair0786786@gmail.com (M.O.Z.); hassantauseef10@gmail.com (T.H.)

* Correspondence: zhasan.biochem@gmail.com

[†] Presented at the 4th International Online Conference on Nanomaterials, 5–19 May 2023; Available online: <https://iocn2023.sciforum.net/>.

Abstract: Recycling plant-based materials for various applications not only reduces the harm to the environment but also presents an excellent green source for nanomaterial synthesis. Being chiral and biodegradable makes cellulose, which is an organic polymer, an economic and easy-to-access plant-derived green material. Cellulose can be synthesized into nanostructures for a vast array of high-demand applications, such as drug delivery; biomedicines, which includes “biosensors and diagnostics”; medical implants; skin tissue healing; wastewater treatment; touch screen technology; electronic skin; human–machine interfaces; flexible devices; energy storage devices; clothes; packaging; and cosmetics. The daily newspapers that are delivered to our homes can be one of the best sources of cellulose for us. Our work in this study concentrated on removing nanocrystalline cellulose from newspapers. To begin, we deinked the newspapers and then the deinked pulp was transformed into its nanostructures, or nanocrystalline cellulose, to achieve a high aspect ratio, on the one hand, using chemicals like NaOH, thiourea, etc., and on the other side, via a mechanical process. We used a variety of characterization techniques, including scanning electron microscopy to study morphological properties, X-ray diffraction, and dynamic light scattering for dimensional analysis, Fourier transforms infrared spectroscopy for thermogravimetric analysis, and others, to confirm that the synthesized materials had achieved the intended outcomes. A high aspect ratio enables us to create surfaces with a huge surface area with very little synthetic material. The final product, which was created by synthesis, has been discovered to have features that are identical to those of nanocrystalline cellulose, which is available for purchase in the market for use in laboratory purposes. To make nanocomposites, this nanocrystalline cellulose can be combined with various organic and inorganic polymers, which can be further used as a base material for energy storage devices. In this paper, we compared our materials at different time durations used in synthesis.

Keywords: synthesis; cellulose; characterization; newspaper; nanomaterials

Citation: Hasan, Z.; Zubair, M.O.; Hassan, T. Synthesis and Characterization of Cellulose Nanomaterials from Waste Newspapers. *Mater. Proc.* **2023**, *14*, 74. <https://doi.org/10.3390/IOCN2023-14731>

Academic Editor: José Luis Arias Mediano

Published: 30 May 2023



Copyright: © 2023 by the authors. Licensee MDPI, Basel, Switzerland. This article is an open access article distributed under the terms and conditions of the Creative Commons Attribution (CC BY) license (<https://creativecommons.org/licenses/by/4.0/>).

1. Introduction

For approximately 150 years, cellulose, the most prevalent renewable and naturally occurring polymer, has been utilized either directly as raw fibers or after being processed [1]. Waste newspapers (WNPs) are being used more effectively as raw materials for a variety of applications because of the depletion of non-renewable resources. Standard waste newspapers (WNPs), which contain inexpensive cellulosic material and make up a good amount of municipal solid waste, are made of biomass resources. All over the world, millions of tons of WNPs are produced and utilized, producing a sizeable amount of wastepaper. As a result of the cellulose content in WNPs, high-value cellulose-based materials made from WNPs can offer an alternate form of recycling.

One of the most plentiful renewable natural resources is cellulose, which is composed of linear linkages between the monosaccharide glucose $(C_6H_{10}O_5)_n$. Cellulose polymers have both crystalline and amorphous areas [2]. Furthermore, cellulose has a long history of use in a wide range of products, including paper, clothing, adhesives, textiles, food, cosmetics, and pharmaceuticals [3]. The separation of nanocellulose from diverse renewable sources and its use in technical applications have drawn more interest in the development of nanotechnology [4,5]. The creation of cellulose nanocrystals (CNCs) using WNPs has recently attracted more attention for research studies. Recent years have seen the publication of several studies utilizing nanocellulose as a reinforcing phase in bio-composite materials [6]. Only a few researchers have used old newspapers or newsprint paper to create nanocellulose; as a result, more understanding in this field is desirable. In this regard, on-site nanocellulose synthesis offers a highly interesting alternative.

Since Ranby initially isolated CNCs in 1951 using cellulose fibers and sulfuric acid hydrolysis, CNCs have gained prominence [7]. In comparison to cellulose fibers, these CNCs have several benefits, including high strength, high surface area, special optical characteristics, lightweight structure, stiffness, etc. Their intrinsic renewability and sustainability have also received significant interest, in addition to their qualities and potential for wide application [8].

One of the promising preparation methods that has been thoroughly researched in the literature is strong sulfuric acid hydrolysis. Acid hydrolysis preferentially targets the disordered cellulose, leaving the crystalline cellulose as the ultimate CNC product. The final CNC result was crystalline cellulose [9]. CNC has certain qualities that make it very desirable for applications that add value, including a high elastic modulus, a profusion of hydroxyl (-OH) groups [10], and chemical reactivity [11]. In numerous possible uses, including those in food, medicine, cosmetics, pulp, paper, reinforcing, and other special function additives, cellulose nanocrystals (CNCs) are emerging as a new material [12].

The WNPs were deinked using a chemical pre-treatment in the current work, which included sodium hydroxide and hydrogen peroxide. The chemical makeup, fiber shape, and brightness of the WNPs were examined to improve the technological conditions for deinking. The CNCs were prepared using carefully controlled sulfuric acid hydrolysis. The processed CNCs were then characterized using techniques such as scanning electron microscopy (SEM), Fourier transform infrared spectroscopy (FTIR), X-ray diffraction (XRD), zeta potentials measurements, and UV-visible spectroscopy for further studies.

2. Materials and Methods

2.1. Materials Used

Waste newspapers (WNPs) from households were taken as raw material. Sodium hydroxide (NaOH), hydrogen peroxide (H_2O_2), sulfuric acid (H_2SO_4), and sodium silicate (Na_2SiO_3) were purchased from Merck (India). All other chemicals used in the study were of analytical grade and purchased from standard agencies.

2.2. Methodology

2.2.1. Deinking of WNPs

Firstly, 20 g of small pieces of WNP were treated with 100 mL of 1.5 M sodium hydroxide, 100 mL of 3 M hydrogen peroxide, and 100 mL of 1 M of sodium silicate together at 50 °C and 1200 rpm for 3 h. The deinked pulp was then filtered and washed with DI water, followed by drying to obtain the sample (T1), as shown in Figure 1.

2.2.2. Preparation of CNCs

CNCs by Chemical Hydrolysis

As represented in Figure 2, CNCs were prepared via the chemical hydrolysis method. The obtained dried WNPs were added into 100 mL of 1 M sulfuric acid at 50 °C, with constant stirring. They were then stirred for 4 h (T2) and 6 h (T3) at 500 rpm and 50 °C. DI water was added in plenty to terminate the reaction of sulfuric acid with WNP pulp,

followed by centrifugation of the suspension to remove the sulfuric acid. The solution was then filtered and washed with DI water until neutralized. The obtained CNCs were then dried and placed under vacuum conditions.

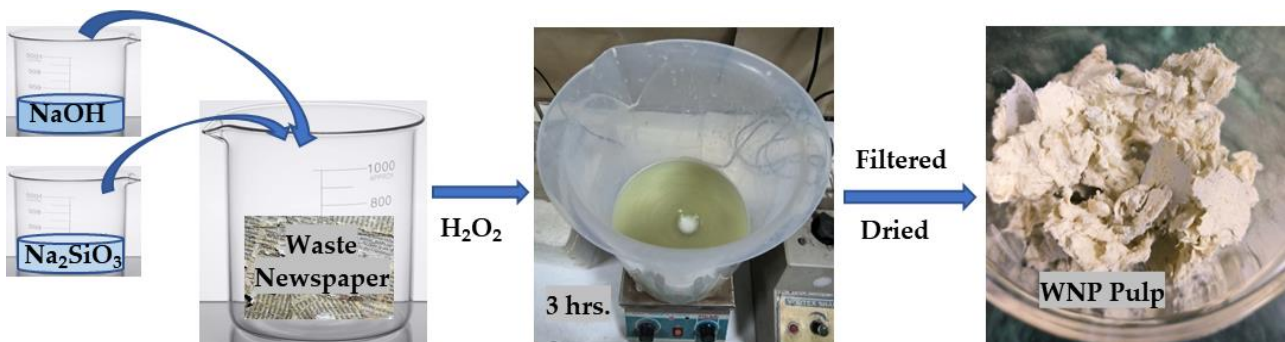


Figure 1. Flow diagram representing extraction of dry WNP pulp from the waste newspaper.

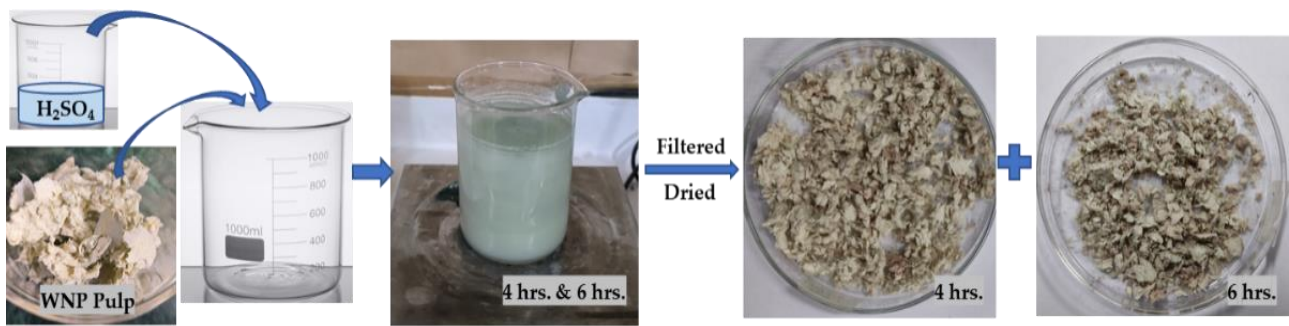


Figure 2. The process design represents acid hydrolysis of WNP pulp for 4 h and 6 h.

CNC by Mechanical Grinding

For this, 1 g of the obtained dried WNPs was mechanically ground by ball milling for 4 h (T4) and 6 h (T5) with 80 g of 0.5 mm porcelain balls to obtain the CNCs.

2.2.3. CNC Characterizations

Scanning Electron Microscopy (SEM)

The surface morphology was examined using SEM (JEOL—JCM 600, 20 kV, Tokyo, Japan). The CNC suspensions were dried for three hours at 50 °C, and the samples were then coated with gold using a scattering apparatus (SCANCOAT, PIRANI 501) under a pressure of 0.3 mbar at 1.5 kV for 35 s.

X-ray Diffraction (XRD)

Graphite monochromators and an auto-divergent slit on a Philips X'Pert MPD X-Ray diffractometer by Philips healthcare (Amsterdam, Netherlands) with Cu-K α radiation operating at 45 kV and 40 mA were used to obtain X-ray diffraction (XRD) spectra. At a scanning rate of 1.5°/min, XRD patterns were captured from 10° to 80°.

Fourier Transforms Infrared Spectroscopy (FTIR)

To determine the chemical makeup of the lignocellulosic components present in the samples, FTIR analysis was used. Frontier 94942 technology was used (PerkinElmer, Waltham, MA, USA). This instrument has a resolution of 2 cm⁻¹. In total, 64 scans were performed using the attenuated total reflectance accessory to record the spectra between 400 and 4000 cm⁻¹.

Dynamic Light Scattering (DLS) and Zeta Potentials Measurements

The estimated crystal size of the nanocellulose distributed in water was determined as the hydrodynamic radius. A dynamic light scattering system (ALV-CGS3) with a fixed 90° scattering angle was used to gather the data. The laser used was a 22 mW HeNe polarized laser with a 633 nm wavelength.

Using a ZetaPALS by Brookhaven Instruments (Holtville, NY, USA), apparatus based on electrophoretic light scattering, the zeta potentials of CNC suspensions were measured. Three measurements were used to average the data, which were performed at a constant 25°C .

UV-Visible Spectroscopic

Spectroscopy in the UV-visible range was used to characterize the CNCs. After diluting the sample with ethanol, the UV-visible spectra of the solutions were measured to determine the number of WNPs that decreased chemically. A UV-vis spectrophotometer was used to monitor the spectra of the CNC solution in the 200–700 nm wavelength range. To change the baseline, ethanol was utilized as a placeholder.

3. Results and Discussion

3.1. Scanning Electron Microscopy (SEM)

Figure 3 displays sample micrographs. They show the exterior aspect's morphology after isolation techniques. The samples' shapes and agglomerations are different from one another in the photographs. The presence of structured regions and the presence of amorphous regions on the surface of the CNC indicates that isolations were only partially effective. Before the examination, the nanostructure suspensions in the CNC-mechanical showed precipitation. It might be a sign that the resulting nanostructures were unstable, and that the precipitation happened because of aggregates being deposited. The introduction of sulfuric acid in the CNC-chemical samples caused the amorphous region to disintegrate and led to the grafting of negatively charged sulfate groups onto the CNC surface. The colloidal suspension was stabilized by repulsive interparticle force thanks to these findings [13,14]. Taking the stability of the nanostructures into consideration, CNC-chemical provided a better result.

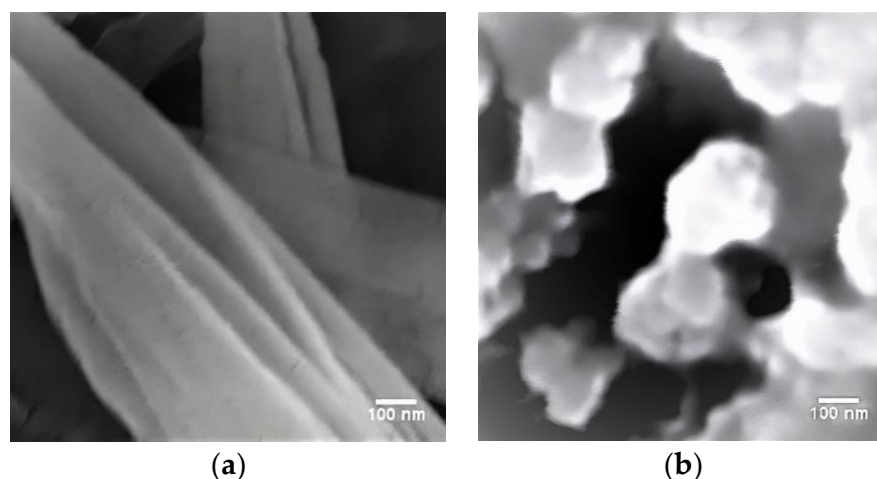


Figure 3. SEM images for (a) CNC-chemical, (b) CNC-mechanical.

3.2. X-ray Diffraction (XRD)

Figure 4a shows the XRD spectra of the hydrolyzed samples, T2 and T3. T2, hydrolyzed for 4 h, had major diffraction peaks at $2\theta = 23.15$ against the lattice plane (002). T2 also showed some smaller peaks. In addition, the T3 sample, hydrolyzed for 6 h, had major diffraction peaks around $2\theta = 23.31$ for the hkl-lattice at (002), and some small peaks were present [15]. The presence of characteristic peaks in XRD for samples T2 and T3 confirms the formation of cellulose, supporting the FTIR analysis.

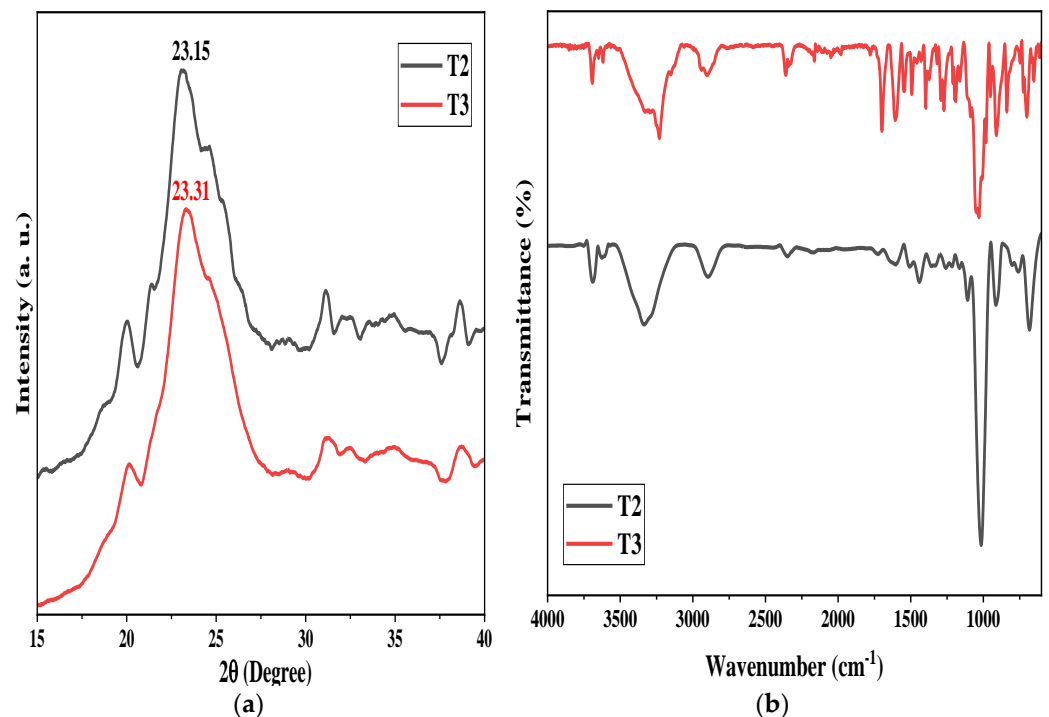


Figure 4. (a) XRD, (b) FTIR for CN-chemical, samples T2 and T3.

3.3. Fourier Transform Infrared Spectroscopy (FTIR)

The FTIR spectra of the samples T2 and T3 are displayed in Figure 4b. It illustrates how the chemical makeup of the fiber changes over time. The modifications in the hydroxyl and carboxyl sections were used to track variations related to the transition from macro- to nanomaterials. The hydroxyl group and aliphatic saturated C-H stretching vibrations of cellulose were responsible for the peaks at around 3336 and 2899 cm^{-1} , which were found in all the samples [16]. The samples' spectra clearly showed the peak at about 1640 cm^{-1} , connected to the O-H bending vibration of absorbed water. Regarding the potential effects of extractions on transmittance bands, smoothed peaks were seen between 1100 and 1500 cm^{-1} , an area where it was impossible to attach signatures for specific vibrations because complicated overlap effects may take place. The hemicelluloses and proteins found in the cellulose fiber walls may also be the cause of these tiny peaks [17]. Each sample had cellulose-typical spectra. The nanocellulose spectra (CNC-chemical (T2, T3)) showed peaks at around 1040 and 910 cm^{-1} , which, according to the literature, indicate the purity of the crystalline band of cellulose and show characteristics of C-O stretching vibration and elongation of cellulose typical pulp-glycoside bonds, respectively [18]. It is significant to notice that the recovered nanocellulose exhibited transmittance signals at around 1428 , 1158 , and 910 cm^{-1} , indicating that the majority of the nanocellulose produced was in the form of the cellulose I structure, which is the form of native cellulose [19]. Thus, the FTIR analysis confirmed the formation of cellulose I in both samples, T2 and T3.

3.4. Dynamic Light Scattering (DLS) and Zeta Potentials Measurements

DLS is a useful tool for approximating the distribution of particle sizes in nanosized materials. In this approach, the CNCs were modelled as spheres in Brownian motion, measuring the particles' hydrodynamic radius (RH) [21], which is equivalent to the translational diffusion coefficient of the particles. The particle size distribution of the CNC-chemical and CNC-mechanical samples is depicted.

Although the potential values were low, i.e., -3.95 mV for T2 and -8.25 mV for T3, as in Table 1, it is evident from the visuals in Figure 5, that there were charges surrounding the droplets. The potential values have a negative sign because of the presence of a negative charge on CNC-chemical because of the grafting, as discussed earlier in SEM. Zeta potential

measurements gave a conductivity for T2 and T3 of 0.388 mS/cm and 0.586 mS/cm, respectively. Higher zeta potential, as well as conductivity, was found for sample T3 as compared to T2.

Table 1. Zeta potential (mV) and conductivity for CNC-chemical, samples T2 and T3.

Samples	Zeta Potential (mV)	Conductivity (mS/cm)
T2	−3.95	0.388
T3	−8.25	0.586

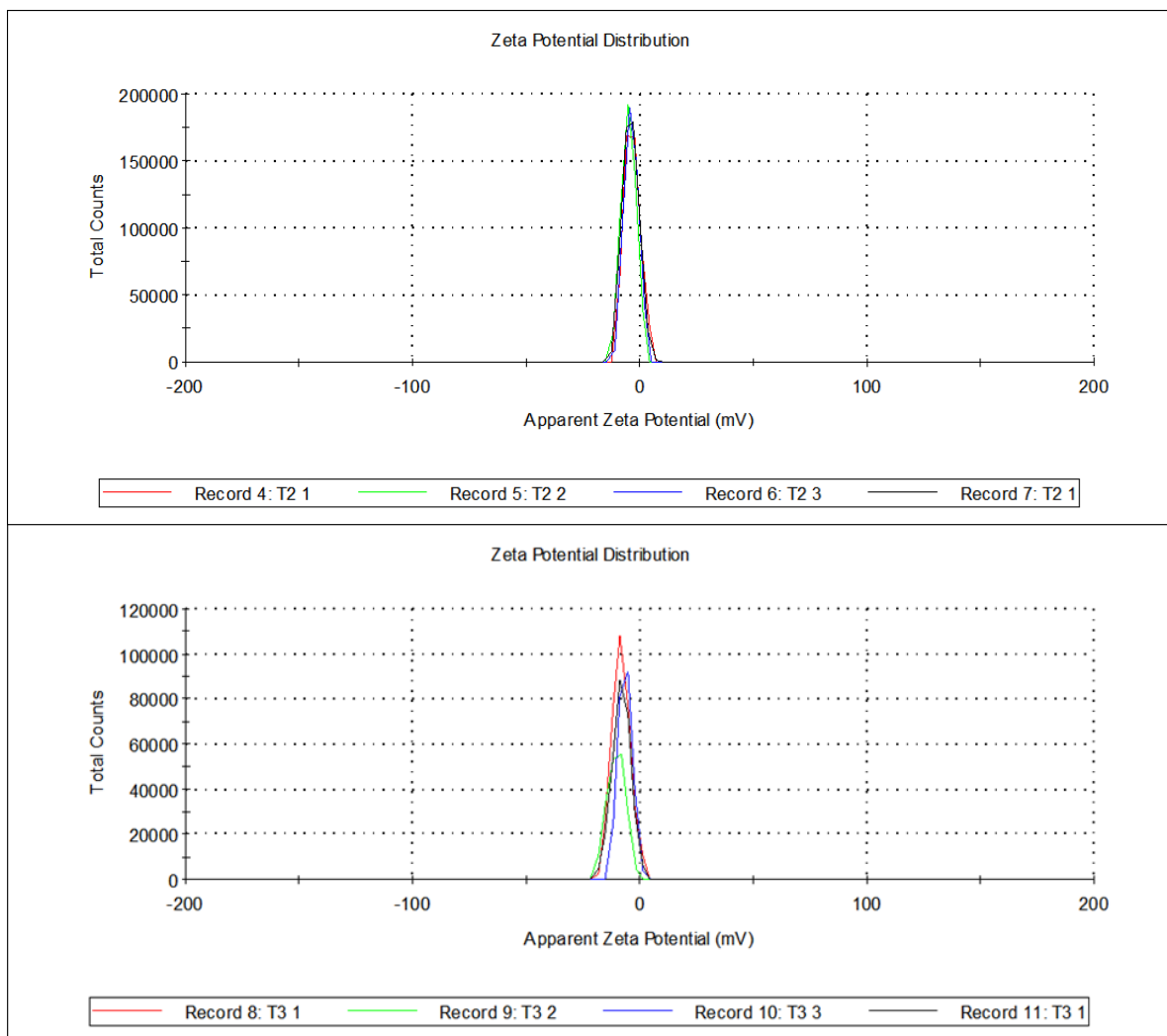


Figure 5. Total counts versus zeta potential (mV) for T2 and T3.

3.5. UV-Vis Spectroscopic Analysis

Studies using UV-Vis (Figure 6) were able to easily distinguish between the T2 and T3 samples. Substantial progress was made. Due to the π^* and $n\pi^*$ excitations of conjugated phenolic groups, T2 exhibited two separate UV peaks (without any shoulders), while T3 had a total of three peaks visible, suggesting superiority. NaOH has a hypochromic effect, which causes the primary absorption, which is typically around 280 nm, to shift to 200–220 nm [20].

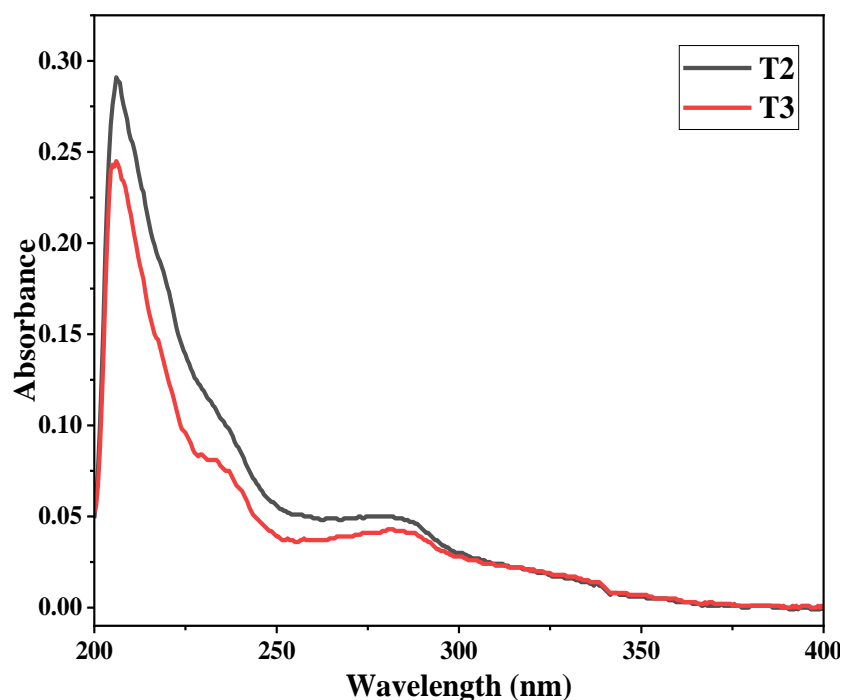


Figure 6. UV-Vis for CNC-chemical samples T2 and T3.

4. Conclusions

In this study, CNCs were isolated from waste newspapers. Firstly, the newspaper was deinked, followed by isolation via chemical and mechanical methods for 4 h and 6 h to study the effect of the time on the as-synthesized material. Observations done by SEM analysis of CNC-chemical and CNC-mechanical samples suggested that both processes give different morphologies and tended to agglomerate. Formation of cellulose was confirmed by FTIR analysis and XRD analysis for T2 and T3. Zeta potential measurements and UV-vis give a better result for T3 as compared to T2, whereby T3 had approximately double values for potential and conductivity as compared to that of T2. Additionally, more peaks were present for T3 in UV-vis as compared to T2. Following analysis of the samples with the help of the above-mentioned characterizations, although CNC-chemical sample T3 seems to be better than other samples, further studies are required to establish this observation.

Author Contributions: Conceptualization, Z.H. and M.O.Z.; methodology, Z.H., M.O.Z. and T.H.; formal analysis, M.O.Z.; investigation, M.O.Z. and T.H.; resources, Z.H.; data curation, T.H. and Z.H.; writing—original draft preparation, M.O.Z.; writing—review and editing, Z.H.; visualization, M.O.Z. and T.H.; supervision: Z.H. All authors have read and agreed to the published version of the manuscript.

Funding: This research received no external funding.

Institutional Review Board Statement: Not applicable.

Informed Consent Statement: Not applicable.

Data Availability Statement: The data presented in this study are available on request from the corresponding author. The data are not publicly available because they are part of the study which will be published in a full-length paper later.

Acknowledgments: Authors are thankful to Central Instrumentation Facility, Jamia Millia Islamia for Instrumentation facilities provided during the study. Z.H. is thankful to Indian Council for Medical Research for awarding the Senior Research fellowship [Sanction No. Myco/Fell./2/2020-ECD-II].

Conflicts of Interest: The authors declare no conflict of interest.

References

1. Mohamed, M.A.; Salleh, W.N.W.; Jaafar, J.; Ismail, A.F.; Abd Mutalib, M.; Mohamad, A.B.; Zain, M.F.M.; Awang, N.A.; Hir, Z.A.M. Physicochemical characterization of cellulose nanocrystal and nanoporous self-assembled CNC membrane derived from *Ceiba pentandra*. *Carbohydr. Polym.* **2017**, *157*, 1892–1902. [[CrossRef](#)] [[PubMed](#)]
2. Morais, J.P.S.; Rosa, M.F.; Filho, M.M.S.; Nascimento, L.D.; Nascimento, D.M.; Cassales, A.R. Extraction and characterization of nanocellulose structures from raw cotton linter. *Carbohydr. Polym.* **2013**, *91*, 229–235. [[CrossRef](#)] [[PubMed](#)]
3. Kallel, F.; Bettaieb, F.; Khiari, R.; García, A.; Bras, J.; Chaabouni, S.E. Isolation and structural characterization of cellulose nanocrystals extracted from garlic straw residues. *Ind. Crop. Prod.* **2016**, *87*, 287–296. [[CrossRef](#)]
4. Campano, C.; Merayo, N.; Balea, A.; Tarrés, Q.; Delgado-Aguilar, M.; Mutjé, P.; Negro, C.; Blanco, Á. Mechanical and chemical dispersion of nanocelluloses to improve their reinforcing effect on recycled paper. *Cellulose* **2018**, *25*, 269–280. [[CrossRef](#)]
5. Campano, C.; Miranda, R.; Merayo, N.; Negro, C.; Blanco, A. Direct production of cellulose nanocrystals from old newspapers and recycled newsprint. *Carbohydr. Polym.* **2017**, *173*, 489–496. [[CrossRef](#)] [[PubMed](#)]
6. Afra, E.; Yousefi, H.; Hadilam, M.M.; Nishino, T. Comparative effect of mechanical beating and nanofibrillation of cellulose on paper properties made from bagasse and softwood pulps. *Carbohydr. Polym.* **2013**, *97*, 725–730. [[CrossRef](#)] [[PubMed](#)]
7. Rånby, B.G. Fibrous macromolecular systems. Cellulose and muscle. The colloidal properties of cellulose micelles. *Discuss. Faraday Soc.* **1951**, *11*, 158–164. [[CrossRef](#)]
8. Habibi, Y. Key advances in the chemical modification of nanocelluloses. *Chem. Soc. Rev.* **2014**, *43*, 1519–1542. [[CrossRef](#)] [[PubMed](#)]
9. Habibi, Y.; Lucia, L.A.; Rojas, O.J. Cellulose nanocrystals: Chemistry, self-assembly, and applications. *Chem. Rev.* **2010**, *110*, 3479–3500. [[CrossRef](#)] [[PubMed](#)]
10. Ng, H.-M.; Sin, L.T.; Tee, T.-T.; Bee, S.-T.; Hui, D.; Low, C.-Y.; Rahmat, A. Extraction of cellulose nanocrystals from plant sources for application as reinforcing agent in polymers. *Compos. Part B Eng.* **2015**, *75*, 176–200. [[CrossRef](#)]
11. Sun, B.; Hou, Q.; Liu, Z.; Ni, Y. Sodium periodate oxidation of cellulose nanocrystal and its application as a paper wet strength additive. *Cellulose* **2015**, *22*, 1135–1146. [[CrossRef](#)]
12. Dong, H.; Strawhecker, K.E.; Snyder, J.F.; Orlicki, J.A.; Reiner, R.S.; Rudie, A.W. Cellulose nanocrystals as a reinforcing material for electrospun poly(methyl methacrylate) fibers: Formation, properties and nanomechanical characterization. *Carbohydr. Polym.* **2012**, *87*, 2488–2495. [[CrossRef](#)]
13. Abraham, E.; Deepa, B.; Pothen, L.; Cintil, J.; Thomas, S.; John, M.; Anandjiwala, R.; Narine, S. Environmental friendly method for the extraction of coir fibre and isolation of nanofibre. *Carbohydr. Polym.* **2013**, *92*, 1477–1483. [[CrossRef](#)] [[PubMed](#)]
14. Nuruddin, M.; Hosur, M.; Uddin, M.J.; Baah, D.; Jeelani, S. A novel approach for extracting cellulose nanofibers from lignocellulosic biomass by ball milling combined with chemical treatment. *J. Appl. Polym. Sci.* **2016**, *133*, 42990. [[CrossRef](#)]
15. Zhang, H.; Ning, Z.; Khalid, H.; Zhang, R.; Liu, G.; Chen, C. Enhancement of methane production from Cotton Stalk using different pretreatment techniques. *Sci. Rep.* **2018**, *8*, 3463. [[CrossRef](#)] [[PubMed](#)]
16. Lani, N.S.; Ngadi, N.; Johari, A.; Jusoh, M. Isolation, Characterization, and Application of Nanocellulose from Oil Palm Empty Fruit Bunch Fiber as Nanocomposites. *J. Nanomater.* **2014**, *2014*, 702538. [[CrossRef](#)]
17. Bellamy, W.D. Single cell proteins from cellulosic wastes. *Biotechnol. Bioeng.* **1974**, *16*, 869–880. [[CrossRef](#)] [[PubMed](#)]
18. Chandra, C.S.J.; George, N.; Narayanankutty, S.K. Isolation and characterization of cellulose nanofibrils from arecanut husk fibre. *Carbohydr. Polym.* **2016**, *142*, 158–166.
19. Chen, Y.W.; Lee, H.V.; Juan, J.C.; Phang, S.-M. Production of new cellulose nanomaterial from red algae marine biomass *Gelidium elegans*. *Carbohydr. Polym.* **2016**, *151*, 1210–1219. [[CrossRef](#)] [[PubMed](#)]
20. Azadi, P.; Inderwildi, O.R.; Farnood, R.; King, D.A. Liquid fuels, hydrogen and chemicals from lignin: A critical review. *Renew. Sustain. Energy Rev.* **2013**, *21*, 506–523. [[CrossRef](#)]

Disclaimer/Publisher’s Note: The statements, opinions and data contained in all publications are solely those of the individual author(s) and contributor(s) and not of MDPI and/or the editor(s). MDPI and/or the editor(s) disclaim responsibility for any injury to people or property resulting from any ideas, methods, instructions or products referred to in the content.